



OPEN Polymethoxyflavones from *Kaempferia parviflora* stimulate melanogenesis by blocking the TPC2 channel

Pattara Pongcho^{1,2,3}, Rachel Tang³, Rita Hairani^{4,10}, Carla Abrahamian^{5,6}, Ponsawan Netcharoensirisuk², Warinthorn Chavasiri⁴, Chatchai Chaotham⁷, Christian Grimm^{3,8,9}✉ & Wanchai De-Eknamkul²✉

Kaempferia parviflora, well-known as Thai ginseng (Krachaidum), has been used as a medicinal plant and food source for centuries. Its rhizome contains several flavonoids, particularly poly-*O*-methylated flavones (also known as polymethoxyflavones). We previously found that *K. parviflora* extract had a strong stimulatory effect on melanogenesis in B16F10 mouse melanoma cells. The aim of this study was to investigate the melanogenic stimulation exerted by various *O*-methylated flavonoids from *K. parviflora* in human melanoma cells and elucidate the mechanism of action of the most active compound. MNT-1 cells were used to screen for the most potent *O*-methylated flavonoid, and its effects on some key steps in melanin biosynthesis would subsequently be investigated. The poly-*O*-methylated flavone 3,5,7,3',4'-pentamethoxyflavone (PMF) exhibited the strongest melanogenesis-stimulating activity among the 13 *O*-methylated flavones isolated from *K. parviflora*. It was shown to enhance tyrosinase (TYR) activity by upregulating the levels of TYR and TYR-related protein 1 (TRP-1) via its inhibitory effect on two-pore channel 2 (TPC2). In conclusion, poly-*O*-methylated flavones, especially PMF, were suggested as a potential group of flavonoids that could stimulate melanin production by inhibiting the activity of the TPC2 channel, leading to increased TYR and TRP-1 activities.

Keywords *Kaempferia parviflora*, Poly-*O*-methylated flavones, 3,5,7,3',4'-pentamethoxyflavone, Melanogenesis, Tyrosinase, TPC2 channel

The human skin, hair, and eyes derive their colours from a pigment called melanin. Melanin is synthesised within specialised cells known as melanocytes, specifically inside intracellular organelles called melanosomes, in a granular form. The melanosomes are subsequently transported and deposited in neighbouring keratinocytes¹. Melanogenesis, the process of producing melanin, is complex, controlled by a network of critical signalling cascades and transcription factors². The various factors involved in melanogenesis can be divided into three groups, namely, the structural proteins of melanosomes, enzymes required for melanin synthesis, and proteins required for melanosome transport and distribution³. Melanocyte dysfunction can disrupt the functions of

¹Pharmaceutical Sciences and Technology Program, Faculty of Pharmaceutical Sciences, Chulalongkorn University, Bangkok 10330, Thailand. ²Department of Pharmacognosy and Pharmaceutical Botany, Faculty of Pharmaceutical Sciences, Chulalongkorn University, Bangkok 10330, Thailand. ³Walther Straub Institute of Pharmacology and Toxicology, Faculty of Medicine, Ludwig Maximilian University, Munich 80539, Germany. ⁴Center of Excellence in Natural Products Chemistry, Department of Chemistry, Faculty of Science, Chulalongkorn University, Bangkok 10330, Thailand. ⁵Department of Cardiology, German Heart Centre, TUM School of Medicine and Health, TUM University Hospital, Technical University of Munich, Munich 80636, Germany. ⁶Partner Site Munich Heart Alliance, German Centre for Cardiovascular Research (DZHK e.V.), 80636 Munich, Germany. ⁷Department of Biochemistry and Microbiology, Faculty of Pharmaceutical Sciences, Chulalongkorn University, Bangkok 10330, Thailand. ⁸Immunology, Infection and Pandemic Research (IIP), Fraunhofer Institute for Translational Medicine and Pharmacology (ITMP), Munich 80333, Germany. ⁹Department of Pharmacology, Faculty of Medicine, University of Oxford, Oxford OX1 3QT, UK. ¹⁰Department of Chemistry, Faculty of Mathematics and Natural Sciences, Mulawarman University, SamarindaEast Kalimantan75123, Indonesia. ✉email: christian.grimm@med.uni-muenchen.de; wanchai.d@chula.ac.th

many pigmentation-related factors that cause hypopigmentation disorder, affecting the colour of the skin, hair, and eyes, as in vitiligo and canities^{4,5}.

Attempts have been made to search for natural products that enhance melanogenic activity in order to overcome hypopigmentation disorders. Plant flavonoids, a group with diverse chemical structures and bioactivities, are of particular interest in this regard. Flavonoids have been classified into many subclasses, including flavonols, flavones, flavanones, isoflavones, chalcones, and anthocyanins, based on the core flavonoid structure. In the literature, flavonoids with melanogenesis-stimulating activity, such as naringenin among the flavanones⁶; quercetin, kaempferol, and rhamnetin among the flavonols^{7–9}; luteolin and chrysin among the flavones⁷; and genistein, pratensein, and dauricin among the isoflavones^{7,10}, have been reported. Among these, naringenin, pratensein, and dauricin have been reported to increase melanin production and tyrosinase (TYR) activity by inhibiting the function of two-pore channel 2 (TPC2) in human MNT-1 cells¹⁰. TPC2 is an ion-transport protein that functions as a counteractive controller of pigmentation by heightening the potential and acidity of the melanosomal membrane^{11–13}.

In addition to the above-mentioned flavonoid diversity, another group of flavones uniquely contains methoxylated substituents; they are methoxylated flavones or *O*-methylated flavones. They have been found in the rhizome extracts of *Kaempferia parviflora*¹⁴. Our research group at Chulalongkorn University has isolated 13 *O*-methylated flavones and completely elucidated their structures based on nuclear magnetic resonance (NMR) spectroscopy analysis¹⁵. We had also previously reported that the extracts of *K. parviflora* and *Dalbergia parviflora* are the only 2 among 40 Thai medicinal plant extracts that exert the strongest effect on stimulating melanin production in B16F10 mouse melanoma cells¹⁰. As little information is available on the effect of *O*-methylated flavones on melanogenesis in human melanocytes, we tested the melanogenesis-enhancing activity of 13 poly-*O*-methylated compounds isolated from the rhizome of *K. parviflora* in human melanoma cells MNT-1. The most potent one was then selected for further in-depth studies to understand the molecular mechanisms involved in melanin synthesis. The findings of this study may contribute to the development of therapeutic agents for hypopigmentation disorders, such as vitiligo, and the formulation of cosmetic products aimed at enhancing skin pigmentation or preventing premature hair greying.

Results

PMF from *K. parviflora* stimulated high melanin production in B16F10 and MNT-1 melanoma cells

Thirteen *O*-methylated flavonoids (KP-1–KP-13) were isolated from the rhizome of *K. parviflora*, as described previously¹⁵. The isolates showed diversity in their structures based on the number and position of the -OCH₃ groups attached to the flavonoid core structure. As shown in Fig. 1a, the -OCH₃ group could be found in the mono- (KP-2, KP-13), di- (KP-1, KP-7, KP-10), tri- (KP-3, KP-5, KP-6, KP-11, KP-12), tetra- (KP-4, KP-8), and even penta-substituted forms (KP-9) of the flavonoids. Among them, three poly-*O*-methylated flavones, namely KP-9 (PMF), KP-7 (DMF), and KP-6 (TMF), were isolated as the major constituents, with high melanogenesis-stimulating activity in both B16F10 mouse melanoma (Fig. 1b) and MNT-1 human melanoma cells (Fig. 1c). PMF was found to be as potent as forskolin, the positive control, followed by DMF and TMF, in both cell types, whereas the other -OCH₃ flavonoids appeared to show lower stimulatory activity. The presence of the two -OCH₃ substituents at positions 5 and 7 of the A-ring (e.g., DMF) was found to be the most important factor for enhancing melanogenic activity. The other -OCH₃ substitutions at position 4' of the B-ring and position 3 of the C-ring seemed relatively less important; however, they did contribute to the enhancement of melanogenic activity, to a certain extent, as seen for PMF. To validate the relationship between the structures and activities

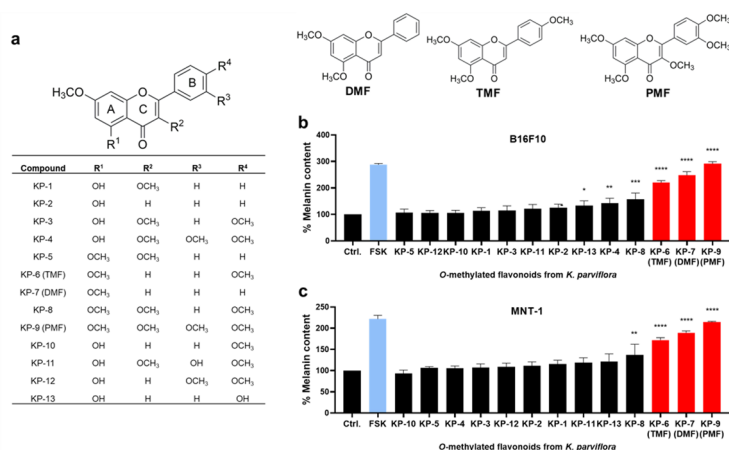


Fig. 1. Structure and melanogenic activity of various *O*-methylated flavonoids isolated from *Kaempferia parviflora*. **(a)** Distribution of -OCH₃ groups in the flavonoids, ranging from mono- to penta-substituted forms. **(b, c)** Melanogenic activity of the isolated *O*-methylated flavonoids in B16F10 and MNT-1 cells. Forskolin was used as a positive control. Data represent means ± SEM from three independent experiments. **p* < 0.05, ***p* < 0.01, ****p* < 0.001, *****p* < 0.0001 vs. control groups.

shown above, we attempted docking of KP-5 to KP-12 into TPC2 using the HADDOCK 2.4 platform. However, despite extensive preprocessing, including ligand energy minimisation, manual PDB editing, and standardisation of residue numbering and atom names, all docking attempts failed at the topology generation step. These issues may have been related to limitations in HADDOCK's compatibility with the chemical complexity of our ligand series and the absence of a high-resolution TPC2–ligand complex structure. Thus, we were unable to generate interpretable docking models. Therefore, PMF was subsequently used to investigate its mechanism of action in MNT-1 human melanoma cells.

PMF enhanced the intracellular TYR activity in MNT-1 cells

Initially, the cytotoxic effect of PMF was evaluated using CellTiter-Blue. MNT-1 cells were treated with PMF (concentration ranging from 1 to 20 μM) for 72 h at 37 $^{\circ}\text{C}$. The results showed that, although PMF at 1–10 μM did not affect the viability of MNT-1 cells, it showed cytotoxicity at 15 and 20 μM , with 79% and 65% cell viability, respectively (Fig. 2a). Thus, the non-toxic concentrations of 1, 5, and 10 μM of PMF were subsequently used for cell treatment. With 10 μM PMF, melanin production in MNT-1 cells increased significantly at 48 and 72 h (Fig. 2b). The effect on melanin production in the cells was dose-dependent, with a maximum increase of 264%, which was comparable to that achieved by the positive control forskolin (FSK) (262%) (Fig. 2c). The negative control treated with 4-butyl resorcinol (TYR inhibitor: TYRi(-)), however, showed a strong decrease in melanin under the same incubation conditions. Similarly, the enzyme activity of TYR in the MNT-1 cells showed the same dose-dependent response to the 10- μM PMF treatment after 72 h of incubation (Fig. 2d).

PMF upregulated the expression of melanogenesis-related proteins in MNT-1 cells

To understand the mechanism underlying the regulation of melanogenesis by PMF, the expression of melanogenesis-related proteins, such as TYR, TYR-related protein 1 (TRP-1), and TYR-related protein 2 (TRP-2) in MNT-1 cells, was examined by western blot analysis. Treatment with PMF at concentrations of 1, 5, and 10 μM for 72 h was found to significantly increase the protein levels of TYR (Fig. 3a) and TRP-1 (Fig. 3b), without affecting the expression of TRP-2 protein (Fig. 3c). For MITF, which is the key transcription factor for pigmentation and the regulation of TYR, TRP-1, and TRP-2 expression, the results were opposite, showing a decrease in the MITF protein level in MNT-1 cells after 72 h (Fig. 3d). In terms of mRNA levels, however, no significant change was observed (Fig. 3e–h). Thus, while the protein expression levels of TYR, TRP-1, and MITF all changed in a dose-dependent manner following PMF treatment, the gene levels did not show significant changes.

PMF enhanced GSK3 β expression and reduced β -catenin levels without affecting the signalling pathways of melanogenesis

The effects of PMF on the expression of various proteins involved in melanogenesis signalling pathways were examined using western blot analysis. The proteins studied included pCREB/CREB, pERK/ERK, pAKT/AKT, GSK3 β , and β -catenin. The results showed that the relative expression levels of pCREB/CREB, pERK/ERK, and pAKT/AKT did not change significantly with increasing PMF concentration (Fig. 4a–c). However, the expression of GSK3 β increased (Fig. 4d), and that of β -catenin decreased (Fig. 4e). This suggests that the

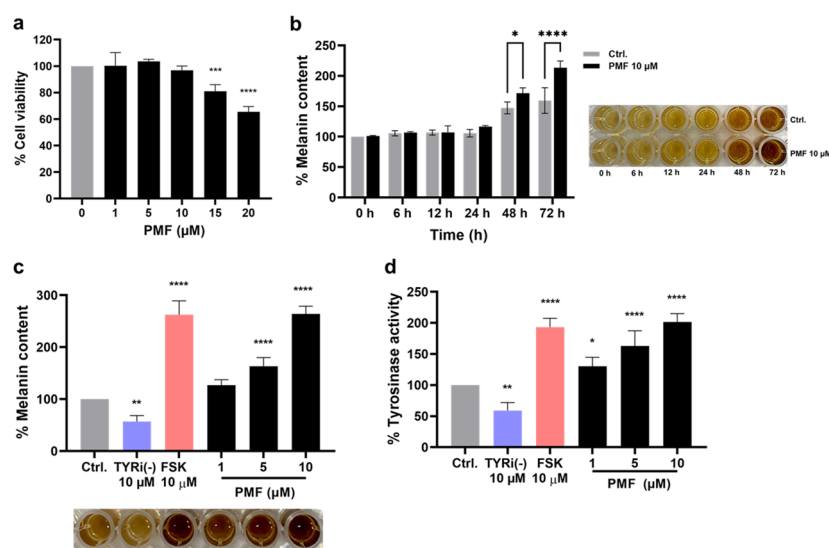


Fig. 2. Effect of PMF on cell viability, melanin production, and TYR activity in MNT-1 cells. **(a)** Cell viability (%) of MNT-1 cells treated with various PMF concentrations for 72 h. **(b)** Effects of PMF (10 μM) on melanin production in MNT-1 cells at different incubation time points. Effect of PMF (1–10 μM) treatment for 72 h on **(c)** melanin production and **(d)** TYR activity in MNT-1 cells. Forskolin was used as a positive control, and 4-butyl-resorcinol (TYRi(-)) served as a negative control. Data represent means \pm SEM from three independent experiments. * $p < 0.05$, ** $p < 0.01$, *** $p < 0.001$, **** $p < 0.0001$ vs. control groups.

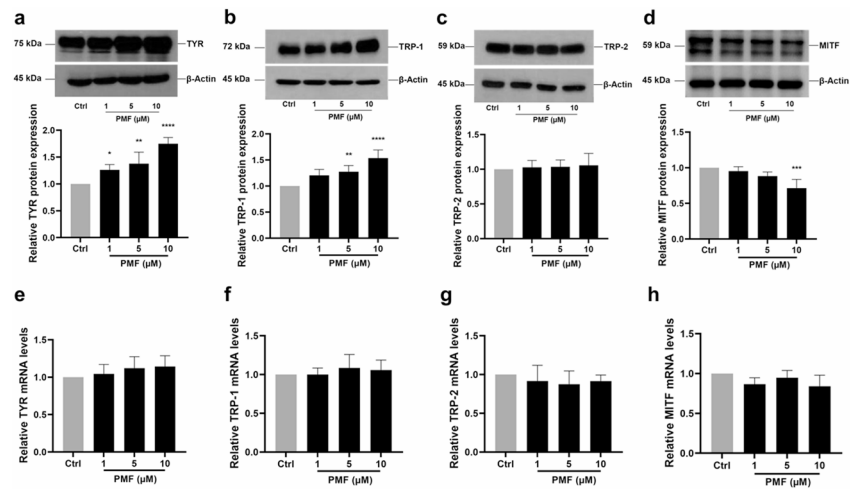


Fig. 3. Effects of PMF on protein and mRNA expression levels of melanogenic proteins in MNT-1 cells. Cells were treated with PMF (1, 5, and 10 μM) for 72 h and western blotting was performed to detect the protein levels of (a) TYR, (b) TRP-1, (c) TRP-2, and (d) MITF. The band intensities were compared with those of the control cells. Real-time PCR analysis of mRNA expression of (e) TYR, (f) TRP-1, (g) TRP-2, and (h) MITF. Data represent means ± SEM from three independent experiments. * $p < 0.05$, ** $p < 0.01$, *** $p < 0.001$, **** $p < 0.0001$ vs. control groups.

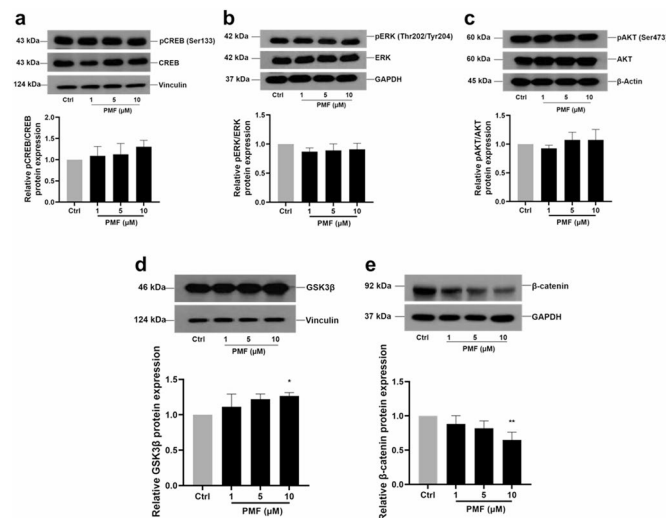


Fig. 4. Effect of PMF on pCREB/CREB, pERK/ERK, pAkt/Akt, GSK3β, and β-catenin protein levels in MNT-1 cells. Cells were treated with PMF (1, 5, and 10 μM) for 72 h and western blotting was performed to detect the protein levels of (a) pCREB/CREB, (b) pERK/ERK, (c) pAkt/Akt, (d) GSK3β, and (e) β-catenin. The band intensities were compared with those of the control cells. Data represent means ± SEM from three independent experiments. * $p < 0.05$, ** $p < 0.01$, *** $p < 0.001$, **** $p < 0.0001$ vs. control groups.

enhanced melanin production induced by PMF may not have occurred through the conventional melanogenesis signalling pathways. However, PMF increased the GSK3β levels while decreasing β-catenin expression, and the elevated GSK3β may have downregulated MITF expression.

PMF inhibited TPC2 channel activity, leading to increased TYR activity, melanin production, and elevated levels of melanogenic protein expression

As shown above, PMF increased the melanin content, TYR activity, and protein expression of TYR and TRP-1 (independently from MITF) without acting via melanogenesis signalling pathways. The upregulation of GSK3β and downregulation of β-catenin (Fig. 4) correlated with the decreased MITF protein levels, likely due to TPC2 loss. As reported by Abrahamian et al., TPC2 promotes the endolysosomal degradation of GSK3β, thereby preventing the proteasomal degradation of MITF¹⁶. Accordingly, TPC2 loss may result in impaired GSK3β degradation, leading to enhanced MITF proteasomal degradation. By conducting endolysosomal patch clamp

experiments with hTPC2 stably overexpressed in HEK293 cells, PMF was found to exert a strong inhibitory effect on hTPC2 (Fig. 5a–c). PMF significantly increased the percentage of TPC2 inhibition (80%), approaching the effectiveness of ATP, a known TPC2 inhibitor (95%). Using the TPC2-knockout MNT-1 cells (MNT-1 TPC2^{-/-}), we confirmed that PMF indeed enhanced melanin production and TYR activity by blocking the TPC2 channel. As shown in Fig. 5d–e, PMF significantly increased melanin production and TYR activity in WT MNT-1 cells. In contrast, when MNT-1 TPC2^{-/-} cells were treated with PMF, no significant difference was observed compared with that in untreated TPC2^{-/-} cells, thereby strongly suggesting that PMF enhanced melanin production and TYR activity by inhibiting TPC2. To confirm the role of TPC2 in PMF-induced melanogenesis, we evaluated the expression of melanogenic proteins in both WT and TPC2^{-/-} MNT-1 cells using 10 μM PMF treatment. PMF treatment significantly increased the levels of TYR and TRP-1 while decreasing MITF expression in the WT MNT-1 cells. Notably, the pattern resembled those of both PMF-treated and untreated TPC2^{-/-} MNT-1 cells (Fig. 5f–h). Additionally, we assessed the mRNA expression of melanogenesis-related genes (MITF, TYR, TRP-1, and TRP-2) following the PMF treatment in both WT and TPC2^{-/-} MNT-1 cells, and observed no significant difference (Fig. S1). To further investigate the upstream regulatory pathways, we examined the expression levels of CREB, ERK, and AKT, and found no significant difference between the WT and TPC2^{-/-} MNT-1 cells (Fig. S2); however, the protein expression of GSK3β increased and that of β-catenin decreased (Fig. 5i–j). Our results strongly suggest that PMF enhanced melanin production and TYR activity by inhibiting TPC2 and regulating GSK3β, β-catenin, and MITF, the latter being the key regulator of melanoma development.

Discussion

The findings of this study show that some poly-*O*-methylated flavones isolated from the rhizome extract of *K. parviflora* exhibit distinct melanogenesis-stimulating effects on both mouse B16F10 and human MNT-1 melanoma cells. The most prominent appeared to be 3,5,7,3',4'-pentamethoxyflavone (PMF), with two methoxy substituents in the A-ring, two in the B-ring, and one in the C-ring. Although the structure–activity relationships were not clear, especially those of compounds KP-5 to KP-12, in silico docking of these methoxyflavones into TPC2 was attempted using the HADDOCK 2.4 platform. Despite extensive preprocessing, including ligand energy minimisation, manual PDB editing, and standardisation of residue numbering and atom names, all docking attempts failed at the topology generation step. These issues may have been related to limitations in the compatibility of HADDOCK with the chemical complexity of our ligand series and the absence of a high-resolution TPC2–ligand complex structure. As a result, we were unable to generate interpretable docking models. However, based on prior in silico studies involving the structurally related flavonoid Naringenin and predicted TPC2 ligand-binding sites, we proposed 12 potential binding sites with varying stability; however, no single definitive binding pockets could be established¹⁷. We also conducted mutagenesis on different residues, finding that the inhibitory effect of naringenin persists, which casts doubt on any single docking hypothesis. Therefore, while naringenin serves as a useful reference, the mechanism of its binding to TPC2 remains ambiguous. We cannot confidently assert a binding mode for PMF based on naringenin. Instead, we hypothesise that PMF may adopt a similar multivalent contact mode (through hydrophobic contacts and methoxy-mediated interactions) across flexible binding regions of the channel. Advances in structural biology, especially ligand-bound cryo-EM or co-crystallography, remain the most promising approach to elucidating the true binding mechanism.

In the literature, many flavonoids have been reported to have melanogenesis-promoting effects. Table S1 summarises various subclasses of flavonoids with melanogenesis-enhancing activity and their potential targets of action. The flavonoid subclasses of flavones and flavonols reported previously mostly contain no methoxy group in the molecules, except for syringetin¹⁸, nobletin¹⁹, tangeretin²⁰, 5-demethylnobletin²¹, and PMF (this study). Interestingly, unlike *O*-methylated flavones, which have been reported to stimulate melanogenesis via conventional pathways, such as CREB activation and ERK signalling, PMF appears to act through a different mechanism. Therefore, this is the first study to demonstrate that PMF from *K. parviflora* exerts its melanogenic effects through TPC2 inhibition; TPC2 is a cation channel localised to both lysosomes and melanosomes. It modulates melanosome maturation, size, and acidity, leading to altered activity of TYR, an enzyme with a highly pH-sensitive function. In this study, we identified naturally derived, low-molecular-weight poly-*O*-methylated flavonoids that selectively enhanced pigmentation via TPC2 inhibition, a significant advance in both mechanism and translational potential.

To further elucidate the melanogenic mechanism of PMF, its effect on melanogenesis-related enzymes was evaluated. PMF increased the expression of TYR and TRP-1, which was consistent with the observed enhancement in melanin synthesis. TRP-2 expression, however, remained unchanged during the same 72-h incubation period. Therefore, our results suggest that PMF enhances melanogenesis by upregulating TYR and TRP-1 without affecting TRP-2. TYR is the key enzyme in melanogenesis, catalysing the production of eumelanin and pheomelanin²², and TRP-1 stabilises TYR and facilitates its transportation to melanosomes; however, TRP-2 plays a less critical role in early melanogenesis^{23–26}.

Although MITF is conventionally considered a key regulator of melanogenesis, the findings of this study demonstrate that PMF treatment induced melanin production in human MNT-1 cells, despite the significant reduction in MITF protein levels. Notably, this reduction did not affect the mRNA levels of MITF or key melanogenic enzymes, including TYR, TRP-1, and TRP-2. Therefore, PMF promotes melanogenesis through an MITF-independent mechanism, potentially by directly modulating downstream melanogenic enzymes or engaging alternative signalling pathways. This observation is consistent with those in previous reports showing that MITF expression is naturally variable in melanoma cells²⁷. Several studies have demonstrated that MITF can be intrinsically downregulated in melanoma cells, including MNT-1 cells, resulting in variability in its levels^{27,28}. In our experiments, PMF treatment led to a further decrease in MITF protein levels. This reduction occurred within a cellular background where MITF was already susceptible to downregulation; thus, PMF may contribute to an environment characterised by intrinsic MITF variability. These findings suggest that the effects of both

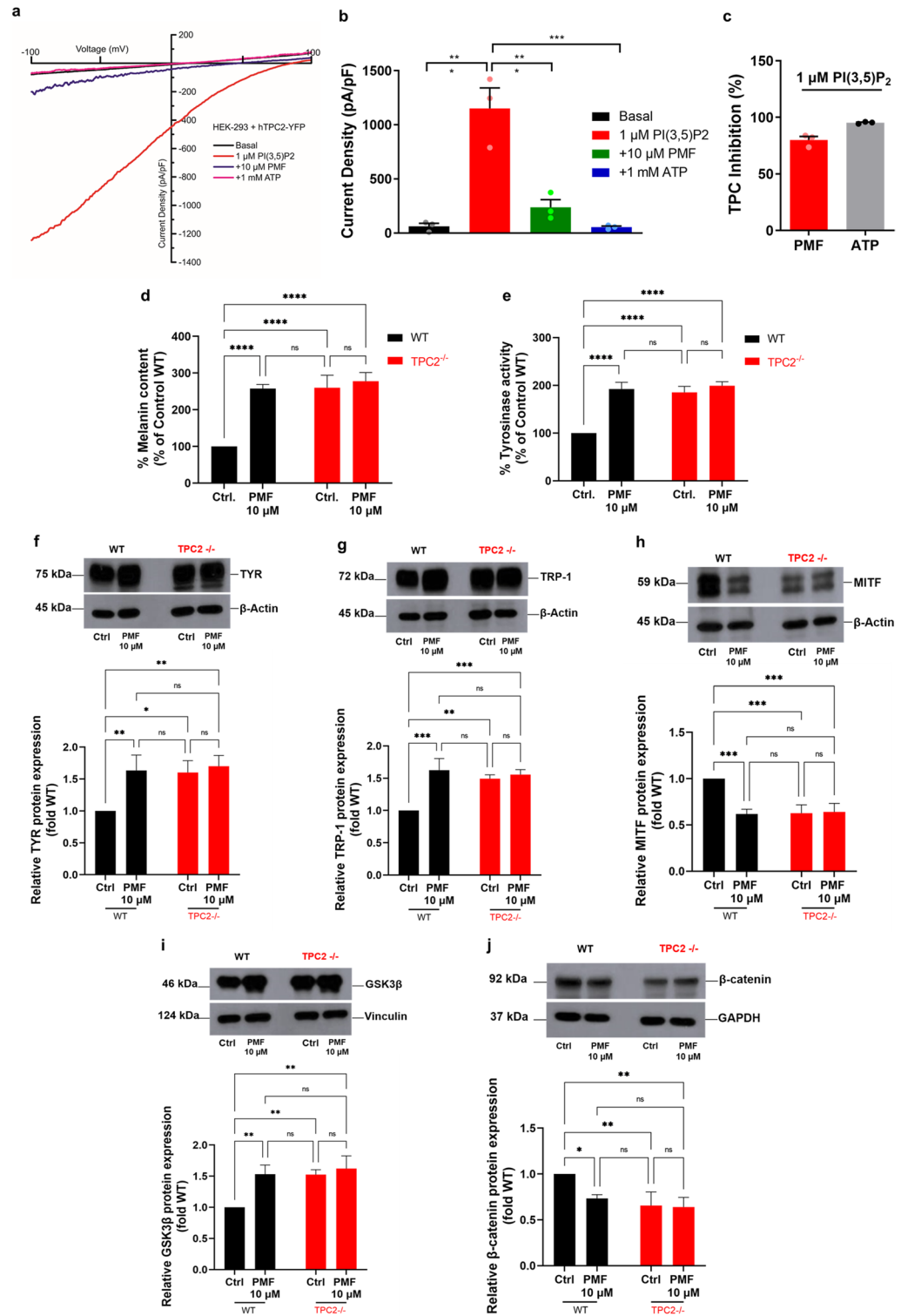


Fig. 5. Inhibition of TPC2 channel activity by PMF. **(a, b)** Representative current density–voltage relations are shown for PMF recordings. **(c)** Inhibition percentages of PMF (10 μM) and ATP (1 mM) as TPC2 blockers upon activation with PI(3,5)P₂ in endolysosomes isolated from HEK293 cells expressing TPC2. MNT-1 WT and TPC2^{-/-} cells were treated with 10 μM PMF for 72 h. Effects of PMF on **(d)** melanin content and **(e)** intracellular tyrosinase activity, and protein expression levels of **(f)** TYR, **(g)** TRP-1, **(h)** MITF, **(i)** GSK3 β , and **(j)** β -catenin detected by western blotting. The bars were compared with the WT MNT-1 cells. Data represent means \pm SEM from three independent experiments. * p < 0.05, ** p < 0.01, *** p < 0.001, **** p < 0.0001 vs. control groups.

PMF-induced melanogenesis through MITF-independent pathways and the intrinsic regulatory characteristics of MNT-1 cells support the existence of MITF-independent mechanisms for melanogenesis in melanoma. Similarly, post-translational regulation of melanogenic enzymes, independent of transcriptional control by MITF, may also be involved in regulating melanogenesis. Such post-translational regulation has been reported to occur independently of MITF^{29,30}. Moreover, the production of the TYR protein depends on proper post-translational modifications and cofactors, with much of its regulation occurring in the ER and Golgi apparatus²⁶.

We also examined upstream signalling pathways regulating MITF expression and found that PMF did not affect the pCREB/CREB, pERK/ERK, and pAkt/Akt protein levels. In contrast, PMF treatment increased GSK3 β expression; therefore, it led to a reduction in the β -catenin levels. This may help to explain the observed reduction in MITF expression. As Wnt signalling stabilises MITF protein levels by inhibiting GSK3 β and promoting the sequestration of GSK3 β -containing destruction complexes into endosomes and multivesicular bodies (MVBs), it prevents GSK3 β from phosphorylating MITF and targeting it for proteasomal degradation, thereby maintaining its stability^{31,32}. The observed dissociation between the unchanged mRNA levels and decreased protein levels of MITF and melanogenic enzymes following PMF treatment suggests regulation at the post-transcriptional or post-translational level. This suggests enhanced proteasomal degradation, altered protein stability, or reduced translation efficiency. MITF is regulated by GSK3 β -mediated phosphorylation, which leads to proteasomal degradation, and may be promoted by PMF treatment. Additionally, melanogenic enzymes such as TYR and TRP-1 depend on post-translational maturation for their stability and function. Interruptions in these processes could further reduce protein levels independently of transcriptional activity. These mechanisms are particularly relevant in melanoma cells, which exhibit high plasticity and rapid protein turnover. Thus, melanogenesis is likely to be regulated through a combination of post-transcriptional mechanisms and alterations in protein stability and expression²⁶.

PMF significantly inhibited TPC2. As shown in Fig. 5, PMF increased melanin production and TYR activity. In addition, PMF elevated TYR and TRP-1, reduced MITF expression, increased GSK3 β , and decreased β -catenin in wild-type MNT-1 cells, resembling the expression patterns observed in both treated and untreated TPC2-knockout MNT-1 cells. These results align with those reported in previous studies. TPC2 is an ion channel localised to both melanosomes and lysosomes, where it regulates organelle membrane potential and luminal pH. In addition, TPC2 modulates pigmentation by controlling melanosome size and acidity; increased melanosomal acidification and membrane potential can suppress the activity of TYR, a pH-sensitive enzyme essential for melanin synthesis^{33,34}. Based on our experimental results, PMF markedly inhibited TPC2. According to Ambrosio et al. (2016), in MNT-1 cells, TPC2 knockout elevated melanosomal pH and increased melanosome size, leading to enhanced melanin production, whereas TPC2 overexpression resulted in decreased melanin levels³³. Our findings are consistent with those of our previous study, which demonstrated that PMF significantly inhibits TPC2. Therefore, it can be proposed that PMF modulates melanogenesis by alkalinising melanosomal pH through TPC2 inhibition, thereby enhancing TYR activity and melanin production.

Notably, TPC2 inhibition or genetic deletion has been shown to promote the proteasomal degradation of MITF without reducing its transcription^{10,16}. In this study, we observed that PMF decreased MITF protein levels without affecting its mRNA, which is consistent with a post-translational mechanism involving TPC2. This effect was previously observed in TPC2 knockout MNT-1 cells, where MITF became more susceptible to proteasomal degradation¹⁰. A plausible mechanism for this is that PMF inhibits the ubiquitin–proteasomal degradation pathway that regulates the rapid turnover of TYR and TRP-1. Supporting this concept, our previous work demonstrated that TPC2 knockout enhanced the proteasomal degradation of MITF itself, as evidenced by its increased sensitivity to cycloheximide and rescue by MG-132 in TPC2 knockout cells. Therefore, TPC2 may play a broader role in controlling the proteasomal turnover of pigmentation-related proteins. Previous work demonstrated that TPC2 knockout led to enhanced proteasomal degradation of MITF in melanocytes, as demonstrated by cycloheximide pulse-chase and rescue with MG-132. This highlights a broader role of TPC2 in regulating the proteasomal turnover of melanogenesis regulators¹⁰. An additional noteworthy aspect is that, in pigmented cells, TRP-1 stabilises the TYR protein and facilitates its transport to melanosomes. Moreover, TYR production relies on post-translational modifications and cofactors, which primarily occur in the endoplasmic reticulum (ER) and Golgi apparatus^{23–25}. This aligns with previous findings that melanin synthesis can be regulated through MITF-independent, post-translational mechanisms. For example, IFNG has been reported to prolong the half-life of TYR by protecting it from proteasomal degradation, thereby enhancing melanin synthesis^{29,30}. These findings suggest that PMF may enhance melanogenesis through post-translational regulation of melanogenic enzymes, particularly by stabilising TYR, independent of MITF-mediated transcriptional control. We therefore propose that PMF mimics this mechanism by inhibiting TPC2, leading to MITF destabilisation and degradation via the proteasome. Thus, PMF likely modulates melanogenesis by alkalinising melanosomal pH through TPC2 inhibition, thereby enhancing the content of melanin and TYR activity. Furthermore, PMF may reduce the risk of melanoma by promoting the proteasomal degradation of MITF, potentially as part of an adaptive feedback response.

TPC2 polymorphisms had been associated with melanogenesis and pigmentation in a previous genome-wide association study³⁵. Very few studies have been conducted on how TPC2 works to control melanogenesis. Ambrosio et al. discovered that TPC2 is expressed in melanosomes and is associated with melanin production. Further, they reported that knocking out TPC2 in MNT-1 cells could increase the pH and size of melanosomes, stimulating melanin synthesis, whereas overexpressing TPC2 led to reduced melanin content³³. In 2017, Chao et al. reported that human polymorphisms, M484L and G734E, which are associated with hypopigmentation and an increased likelihood of blond hair, are gain-of-function (GOF) variations¹¹, and in 2023, another GOF variant, R210C, was discovered in a Chinese proband with blond hair, hypopigmentation, and albinism¹⁵. In 2024, Zhou et al. confirmed that TPC2 is essential for sAC-dependent regulation of melanosomal pH and melanin synthesis. Further, they found that the TPC2 inhibitor Ned19 significantly increased melanosomal pH

and melanin synthesis in both wild-type melanocytes and those with lost sAC activity³⁶. The findings suggested that TPC2 may have been a new target that interferes with melanogenic regulation. Notably, few studies have been conducted on the use of natural compounds as TPC2 blockers in the context of melanogenesis. Our previous study demonstrated the potential of the natural isoflavonoids MT-8 (pratensein) and UM-9 (duartin) in blocking TPC2 activity¹⁰. Loss of TPC2 was found to increase melanin levels and decrease MITF-driven melanoma through the activation of GSK3 β -mediated MITF degradation. A recent study by Abrahamian et al. confirmed that TPC2 knockout decreases MITF levels by increasing GSK3 β expression and preventing β -catenin translocation to the nucleus. This enhances MITF proteasomal degradation, which is significant as MITF overexpression can contribute to melanoma progression¹⁶.

Given its natural origin, favourable safety profile, and ability to modulate pigmentation, PMF holds significant translational potential, both as a pigmentation-enhancing agent for hypopigmentation disorders and as a drug that could be used along with chemotherapeutics to limit melanoma growth through the downregulation of MITF-driven oncogenic programs. Future *in vivo* studies should evaluate the efficacy, safety, and pharmacokinetics of PMF, as well as its potential effects on tumour suppression and skin homeostasis, considering both mechanistic and clinical perspectives. Recent *in vivo* studies have shown that the genetic ablation or inhibition of TPC2 leads to profound suppression of tumour growth and dissemination. First, Abrahamian et al. demonstrated that TPC2 knockout in murine melanoma B16F10-luc cells significantly reduced tumour burden, metastasis, and MITF/ β -catenin expression following subcutaneous injection in C57BL/6 mice, compared with control mice¹⁶. Similarly, Müller et al. (2021) developed two small molecules, SG005 and SG094, derived from the bisbenzylisoquinoline alkaloid in *Stephania tetrandra*. These compounds were found to inhibit TPC2 function and exhibited potent anti-tumour effects, highlighting their potential as therapeutic agents targeting TPC2 in cancer. They reported that TPC2 inhibition nearly stopped tumour growth in a hepatocellular carcinoma model, resulting in a 99% reduction in the bioluminescence signal by day 10³⁷. These findings further highlight TPC2 as a therapeutic target in cancer, particularly melanoma, due to its localisation to melanosomal membranes. Notably, the use of natural compounds as TPC2 inhibitors in this context remains largely unexplored. Naringenin, a natural flavonoid found in citrus fruits and tomatoes, inhibits TPC2 and suppresses NAADP-induced Ca²⁺ signalling, thereby reducing VEGF-driven angiogenesis in both endothelial cells and murine models³⁸. It has also been reported to stimulate melanin production in B16F10 melanoma cells. Other natural isoflavonoids, such as MT-8 (pratensein) and UM-9 (duartin), effectively inhibit TPC2 activity and enhance both melanin synthesis and tyrosinase activity¹⁰. As reported above, TPC2 inhibitors that also stimulate melanin synthesis, such as naringenin, often require high concentrations, with a dosage range of 150 to 900 mg found to be safe for healthy adults, but potentially causing off-target effects^{39,40}. In contrast, PMF offers a potentially safer and more selective alternative. Its ability to act at low concentrations while simultaneously promoting pigmentation and suppressing oncogenic signalling positions it as a promising candidate for future therapeutic development in both dermatological and oncological contexts.

In summary, our findings suggest that PMF functions via two distinct mechanisms: (1) enhancing melanogenesis by increasing the melanin content and TYR activity through a TPC2-dependent pathway, and (2) potentially reducing the risk of melanoma by facilitating the proteasomal degradation of MITF, as summarised in Fig. 6. Importantly, MITF overexpression could lead to melanoma development. Identifying natural compounds that decrease TPC2 activity and increase melanin production would thus be a promising direction for future melanoma research. While further investigation is warranted to fully understand the mechanisms underlying TPC2 and PMF-induced melanogenesis, one possible explanation would be that PMF enhances melanin production independent of MITF by directly interacting with TYR activity in melanosomes. Thus, PMF affects the production of melanin and reduces the risk of melanoma. However, this study has certain limitations. The experiments were conducted *in vitro*, and their findings may not fully reflect *in vivo* conditions. The precise interaction between PMF and TPC2 at the molecular level remains unclear, and potential off-target effects of PMF have not been assessed. *In silico* approaches should be followed to validate the interaction. In addition, further mechanistic studies using more poly-*O*-methylated flavones in addition to PMF (KP-9) would offer more insight into the observed melanogenic activities. The significance of our study lies not only in confirming the role of TPC2 in melanogenesis, but also in providing an *in vitro* proof-of-concept for TPC2 modulation by bioactive dietary compounds, laying the groundwork for the future development of targeted therapies in pigmentation disorders and melanoma.

Methods

Chemicals and reagents

Synthetic melanin, forskolin, and Triton X-100 were purchased from Sigma-Aldrich (St. Louis, MO, USA). Bovine serum albumin, dimethyl sulfoxide, and RIPA lysis buffer were purchased from Merck Millipore (Billerica, MA, USA). Laemmli sample buffer (4 \times), Precision plus protein™ westernC™ blotting standards, Precision protein™ streptactin–HRP conjugate, 40% acrylamide, tetramethylethylenediamine, sodium dodecyl sulphate (SDS), resolving gel buffer, stacking gel buffer, polyvinylidene difluoride membranes, 10 \times Tris/Tricine/SDS buffer, 10 \times Tris/Glycine buffer, and 10 \times Tris buffered saline were purchased from Bio-Rad (Hercules, CA, USA). Tween 20 was purchased from LOBA (Chemie, Mumbai, India). The protease inhibitor cocktail and phosphatase inhibitor were from Roche (Basel, Switzerland). ECL substrate (HRP) superSignal West Pico PLUS was purchased from Thermo Scientific (Rockford, IL, USA). The BCA protein assay kit, PureLink™ RNA mini kit, and RevertAid first-strand cDNA synthesis kit were purchased from Thermo Fisher Scientific (Waltham, MA, USA).

Preparation of *K. parviflora* extracts and isolation of methoxylated flavone constituents

K. parviflora rhizomes, locally cultivated in Phu Ruea, Loei Province, Thailand (17°27'18"N, 101°21'48"E/17.45500°N, 101.36333°E), were obtained from the Thai drug store Chao-Krom-Per in Bangkok.

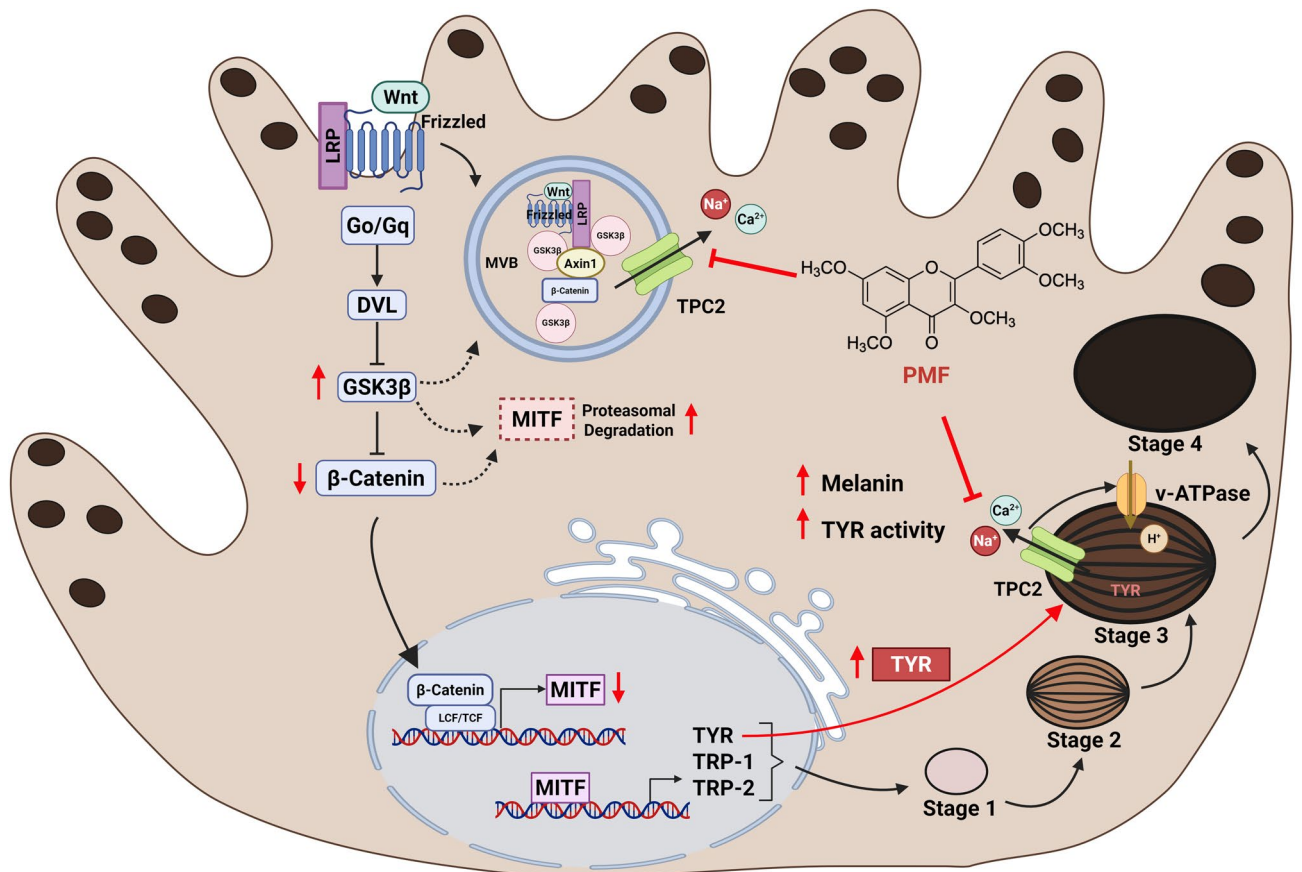


Fig. 6. Schematic illustration of the proposed mechanism of melanogenesis regulation by PMF. PMF enhances melanin production independent of MITF by directly affecting tyrosinase activity, which is pH-dependent and regulated by TPC2 in melanosomes. Inhibition of the TPC2 channel in endolysosomes and melanosomes promotes GSK3 β upregulation and prevents β -catenin translocation to the nucleus, leading to suppressed MITF expression and enhanced proteasomal degradation, along with increased tyrosinase activity and melanin production. “Created in BioRender. Pongcho, P. (2025) <https://BioRender.com/ubtttd9f>”.

The plant material was both identified and deposited (voucher specimen no. 013201, BCU) at the Professor Kasin Suvatabhandhu Herbarium, Department of Botany, Faculty of Science, Chulalongkorn University, Bangkok, Thailand. No specific permissions or licences were required, as the species is not classified as protected under the regulations of Thailand.

Extraction and isolation of various methoxylated flavones from the rhizome of *K. parviflora* were performed using a previously described method¹⁵. For the isolation of the three main constituents, namely 5,7-dimethoxyflavone (DMF), 5,7,4'-trimethoxyflavone (TMF), and 3,5,7,3',4'-pentamethoxyflavone (PMF), the dried rhizome powder (1.1 kg) was extracted with MeOH using a Soxhlet apparatus. After filtration and removal of MeOH in vacuo, the obtained crude MeOH extract was suspended in water and extracted with dichloromethane (CH₂Cl₂). After removing the solvent, the CH₂Cl₂ fraction (39 g) was separated by vacuum column chromatography over silica gel on a sintered glass funnel to provide 12 fractions via TLC profiles. Using Sephadex LH-20 column chromatography and eluted with CHCl₃:MeOH (1:1), DMF (0.9 g) and PMF (1.0 g) were obtained from fraction 9, whereas TMF (0.4 g) was obtained from fraction 10. Using HPLC, the purity of these compounds was determined to be $\geq 98\%$.

Cell cultures

Human melanoma cell lines (WT MNT-1) were acquired from the American Type Culture Collection (ATCC, Manassas, VA, USA). MNT-1 knockout cells (TPC2^{-/-} KO) were established as reported previously¹⁰. Both cell types were cultured in DMEM containing 20% FBS, 10% AIM-V medium, and 1% antibiotic-antimycotic solution. For patch-clamp experiments, human embryonic kidney HEK293 cells (sourced from DSMZ, Braunschweig, Germany) were utilised. HEK293 cells were cultured in DMEM supplemented with 1 g/L of glucose, 100 U/mL of penicillin-streptomycin, and 10% FBS. The detachment of all cell types from the culture plates was achieved using Trypsin-EDTA (1 \times) and standard cultivation conditions were maintained at 37 $^{\circ}$ C with 5% CO₂ until the cells reached 70–80% confluence for subsequent experiments. All cell culture reagents were purchased from Gibco, Manassas, USA.

Cytotoxicity assay

MNT-1 cells were seeded at a density of 5×10^3 cells/mL in a 96-well plate and incubated overnight for adherence. After treatment with PMF at different concentrations, 20 μ L of CellTiter-Blue reagent (Promega, Mannheim, Germany) per 100 μ L of medium was added to the cells, and incubation continued for 4 h at 37 °C. The fluorescent product, which reflects the number of viable cells, was estimated using a microplate reader at 560 nm excitation and 590–600 nm emission (560 Ex/590–600 Em). Ex/590Em (CLARIOstar, Ortenberg, Germany).

Measurement of melanin production in B16F10 cells

Mouse melanoma cell lines (B16F10) were acquired from the American Type Culture Collection (ATCC, Manassas, VA, USA). B16F10 mouse melanoma cells were cultured in DMEM without phenol red, containing 10% FBS, 1% antibiotic–antimycotic, and 1% GlutaMAX. The cells were seeded at a density of 5×10^3 cells/mL in a 96-well plate (total 200 μ L per well) and incubated overnight for adherence at 37 °C. Non-toxic concentrations (10 μ M) of various test compounds were added to the cells. After 48 h, melanin production was measured using a microplate reader (CLARIOstar, Ortenberg, Germany) at a wavelength of 405 nm. The melanin content was then calculated as follows:

$$\text{Melanin content (\%)} = (A_{\text{sample}}/A_{\text{control}}) \times 100 \quad (1)$$

Measurement of melanin production in MNT-1 cells

Human WT and TPC2^{-/-} KO MNT-1 cells were cultured in 6-well plates at a density of 1×10^5 cells/mL with a medium volume of 2 mL and incubated overnight for adherence. The cells were treated with PMF (1–10 μ M) and forskolin (10 μ M) for 72 h. The cell culture medium was then removed, and the cells were then washed twice with PBS and lysed with 10% RIPA lysis buffer (Merck Millipore, Billerica, MA, USA) supplemented with 1% protease inhibitor cocktail and 1% phosphatase inhibitor (Roche, Basel, Switzerland). The lysed cells were incubated for 45 min in a lysis buffer and centrifuged at 12,000 rpm and 4 °C for 15 min. The supernatant was collected to quantify the protein content using a BCA protein assay kit (Thermo Fisher Scientific, Waltham, MA, USA).

The cell pellets were separately dissolved with a mixture of 1 N NaOH and 10% dimethyl sulfoxide at 100 °C for 3 h. After centrifugation (Axygen, Union City, CA, USA) at 12,000 rpm and 25 °C for 10 min, the supernatants were transferred to a 96-well plate, and melanin content was measured with absorbance at 405 nm using a microplate reader (CLARIO star, Ortenberg, Germany). The quantity of melanin was then compared with the established standard curve for melanin. The melanin content was normalised with the protein amount and expressed either as micrograms of melanin per microgram of protein or as the percentage of the control.

Intracellular TYR activity assay

Enzyme activity was determined in both compound-treated WT MNT-1 and TPC2^{-/-} KO MNT-1 cells. The cells (1×10^5 cells/mL) were seeded and treated either with PMF (1–10 μ M) or forskolin (10 μ M, as the positive control). After 72 h, the cells were washed twice with PBS, collected using a cell scraper, and lysed in 0.1 M PBS at pH 6.8 containing 1% Triton X-100 (Sigma-Aldrich, St. Louis, MO, USA), 1% protease inhibitor cocktail, and 1% phosphatase inhibitor. The lysed cells were mixed using a vortex and then frozen at –80 °C for 5 min, followed by a process of freezing and thawing every 15 min for a total of 3 cycles. Thereafter, the obtained cell suspensions were centrifuged (Axygen, Union City, CA, USA) at 12,000 rpm and 4 °C for 15 min. The supernatants were collected, and the amount of protein was determined using a BCA assay. An equal amount (100 μ g) of protein from each sample (used as the source of the TYR enzyme) was added to a 96-well plate and adjusted to 50 μ L using 0.1 M PBS at pH 6.8. Subsequently, 50 μ L of fresh 2.5-mM L-DOPA was added as a substrate for TYR, followed by further incubation at 37 °C for 2 h, and the absorbance of the resulting dopachrome was measured at 475 nm using a microplate reader.

Western blotting

The protein expression of TYR, TRP-1, TRP-2, MITF, CREB, ERK, AKT, and GSK3 β was studied using western blot analysis. Both WT MNT-1 and TPC2^{-/-} KO MNT-1 cells (1×10^5 cells/mL) were seeded in 6-well plates and incubated at 37 °C for 72 h with PMF (1–10 μ M). Equal amounts of protein lysate and 4 \times Laemmli sample buffer were mixed and heated for 10 min at 95 °C. Protein samples (30 μ g/lane) were separated on a 10% SDS-PAGE and transferred to an Immun-Blot polyvinylidene difluoride membrane. The membranes were blocked with 5% bovine serum albumin in 0.1% TBST for 1 h at 25 °C, and then incubated with primary antibody overnight at 4 °C, washed thrice with TBST for 5 min each, and incubated with secondary antibodies for 1 h. The membranes were then washed thrice with TBST for 5 min each. The signals from a specific protein were then visualised using the chemiluminescent HRP substrate (ECL), and the band intensities were analysed using ImageJ 1.54 software. The antibodies used are listed in Supplementary Table S2.

Real-time PCR

Both WT and TPC2^{-/-} KO MNT-1 cells (1×10^5 cells/mL) were seeded in 6-well plates and treated with PMF (1–10 μ M). Total RNA was extracted from the cells using a PureLink™ RNA mini kit (Thermo Fisher Scientific, Waltham, MA, USA). cDNA was synthesised using a RevertAid first-strand cDNA synthesis kit (Thermo Fisher Scientific). The mRNA expression level of the gene related to melanogenesis was analysed using real-time quantitative reverse transcription PCR (qRT-PCR), performed with a C100 Thermal Cycler (Bio-Rad CFX384 real-time PCR system). Equal amounts of cDNA were amplified using Luna™ Universal qPCR Master Mix (M3003) (Biolab, London, England). The specific forward and reverse primers used are listed in Table S3.

Endolysosomal patch-clamp experiments

Endolysosomal patch-clamp experiments were performed as described previously¹¹. Briefly, HEK293 cells were seeded in a 24-well plate containing poly-L-lysine (Serva)-coated coverslips, where the cell density reached 60–70% confluence for transfection. Cells were transiently transfected with human TPC2-YFP (C-terminally tagged) using TurboFect Transfection Reagent (Thermo Fisher Scientific, Waltham, MA, USA). After 12–24 h of transfection, HEK293 cells were treated overnight with 1 mM Apilimod (Axon Medchem, Groningen, Netherlands) to enlarge lysosomes and late endosomes. TPC2 was activated with 1 μ M PI(3,5)P₂-di8 (Echelon Biosciences, Utah, USA) and inhibited with 1 mM ATP-Mg (Sigma-Aldrich, St. Louis, MO, USA) or PMF 10 μ M. The PI(3,5)P₂-di8, ATP-Mg, or PMF was washed out before patch-clamp experiments were performed. All the currents measured were recorded using an EPC-10 patch-clamp amplifier and PatchMaster software, version v2 \times 90.4 (HEKA Elektronik GmbH, Lambrecht/Pfalz, Germany). Recording pipettes were polished with 4–6 M Ω resistance. The liquid junction potential was corrected. All experiments were conducted at room temperature (23–25 °C). The cytoplasmic solutions were replaced after the application of the agonists or antagonists. Individual ramp current recordings were extracted at a current amplitude of –100 mV. The extracellular/bath solution consisted of 140 mM K-MSA, 5 mM KOH, 4 mM NaCl, 0.39 mM CaCl₂, 1 mM EGTA, and 10 mM HEPES (pH 7.2 was adjusted with KOH); 300 mOsm was adjusted with D-(+)-glucose. The pipette/luminal solution contained 140 mM Na-MSA, 5 mM K-MSA, 2 mM Ca-MSA, 1 mM CaCl₂, 10 mM HEPES, and 10 mM MES (pH 4.6 was adjusted with methanesulfonic acid). In all experiments, 500-ms voltage ramps from –100 to +100 mV were applied every 5 s. Data and statistical analyses of the recordings were conducted using Origin 9 software (OriginLab Corporation, Northampton, MA, USA).

Statistical analysis

All data were obtained from three independent experiments and are presented as the mean \pm standard error of the mean (\pm SEM). Differences between group means were analysed using one-way or two-way analysis of variance (ANOVA), followed by Bonferroni's post hoc test, in GraphPad Prism version 9.0 (GraphPad Software, San Diego, CA, USA). A p-value of <0.05 was considered statistically significant.

Data availability

All data generated or analysed during this study are included in this published article and its supplementary information files.

Received: 17 May 2025; Accepted: 5 November 2025

Published online: 18 November 2025

References

- Cichorek, M., Wachulska, M., Stasiewicz, A. & Tymińska, A. Skin melanocytes: biology and development. *Postepy Dermatol. Alergol.* **30**, 30–41. <https://doi.org/10.5114/pdia.2013.33376> (2013).
- García-Borrón, J. C. & Olivares Sánchez, M. C. in *Melanins Melanosomes* 87–116 (2011).
- Yamaguchi, Y. & Hearing, V. J. Melanocytes and their diseases. *Cold Spring Harb Perspect. Med.* <https://doi.org/10.1101/cshperspect.a017046> (2014).
- Nicolaïdou, E. & Katsambas, A. D. Pigmentation disorders: hyperpigmentation and hypopigmentation. *Clin. Dermatol.* **32**, 66–72. <https://doi.org/10.1016/j.clindermatol.2013.05.026> (2014).
- Sehrawat, M., Sinha, S., Meena, N. & Sharma, P. K. Biology of hair pigmentation and its role in premature canities. *Pigment Int.* **4**, 7–12. <https://doi.org/10.4103/2349-5847.208297> (2017).
- Ohguchi, K., Akao, Y. & Nozawa, Y. Stimulation of melanogenesis by the citrus flavonoid naringenin in mouse B16 melanoma cells. *Biosci. Biotechnol. Biochem.* **70**, 1499–1501. <https://doi.org/10.1271/bbb.50635> (2006).
- Takekoshi, S., Nagata, H. & Kitatani, K. Flavonoids enhance melanogenesis in human melanoma cells. *Tokai J. Exp. Clin. Med.* **39**, 116–121 (2014).
- Mitsunaga, T. & Yamauchi, K. Effect of Quercetin derivatives on melanogenesis stimulation of melanoma cells. *J. Wood Sci.* **61**, 351–363. <https://doi.org/10.1007/s10086-015-1476-9> (2015).
- Tang, H. et al. Kaempferol, the melanogenic component of *Sanguisorba officinalis*, enhances dendricity and melanosome maturation/transport in melanocytes. *J. Pharmacol. Sci.* **147**, 348–357. <https://doi.org/10.1016/j.jpsh.2021.08.009> (2021).
- Netcharoensirisuk, P. et al. Flavonoids increase melanin production and reduce proliferation, migration and invasion of melanoma cells by blocking endolysosomal/melanosomal TPC2. *Sci. Rep.* **11**, 8515. <https://doi.org/10.1038/s41598-021-88196-6> (2021).
- Chao, Y. K. et al. TPC2 polymorphisms associated with a hair pigmentation phenotype in humans result in gain of channel function by independent mechanisms. *Proc. Natl. Acad. Sci. USA* **114**, E8595–E8602. <https://doi.org/10.1073/pnas.1705739114> (2017).
- Patwardhan, A. & Delevoye, C. Ions switch off darkness: role of TPC2 in melanosomes. *Pigment Cell. Melanoma Res.* **29**, 498–499. <https://doi.org/10.1111/pcmr.12510> (2016).
- Wang, Q. et al. A gain-of-function TPC2 variant R210C increases affinity to PI(3,5)P₂ and causes lysosome acidification and hypopigmentation. *Nat. Commun.* **14**, 226. <https://doi.org/10.1038/s41467-023-35786-9> (2023).
- Chen, D., Li, H., Li, W., Feng, S. & Deng, D. *Kaempferia parviflora* and its methoxyflavones: chemistry and biological activities. *Evid. Based Complement. Alternat Med.* **2018**, 4057456. <https://doi.org/10.1155/2018/4057456> (2018).
- Sawasdee, P., Sabphon, C., Sitthiwongwanit, D. & Kokpol, U. Anticholinesterase activity of 7-methoxyflavones isolated from *Kaempferia parviflora*. *Phytother Res.* **23**, 1792–1794. <https://doi.org/10.1002/ptr.2858> (2009).
- Abrahamian, C. et al. Rab7a is an enhancer of TPC2 activity regulating melanoma progression through modulation of the GSK3 β / β -Catenin/MITF-axis. *Nat. Commun.* **15**, 10008. <https://doi.org/10.1038/s41467-024-54324-9> (2024).
- Minicocci, V. et al. A commentary on the Inhibition of human TPC2 channel by the natural flavonoid naringenin: Methods, experiments, and ideas. *Biomol. Concepts.* **14** <https://doi.org/10.1515/bmc-2022-0036> (2023).
- Han, H. & Hyun, C. G. Syringetin promotes melanogenesis in B16F10 cells. *Int. J. Mol. Sci.* **24** <https://doi.org/10.3390/ijms24129960> (2023).
- Yoon, H. S. & Kim, I. J. Nobiletin induces differentiation of murine B16/F10 melanoma cells. *J. Korean Soc. Appl. Biol. Chem.* **54**, 353–361 (2011).

20. Yoon, H. S. et al. Tangeretin triggers melanogenesis through the activation of melanogenic signaling proteins and sustained extracellular Signal-Regulated kinase in B16/F10 murine melanoma cells. *Nat. Prod. Commun.* **10** (3), 389–392. <https://doi.org/10.1177/1934578x1501000304> (2015).
21. Wang, H. M. et al. Natural citrus Flavanone 5-demethylnobiletin stimulates melanogenesis through the activation of cAMP/CREB pathway in B16F10 cells. *Phytomedicine* **98**, 153941. <https://doi.org/10.1016/j.phymed.2022.153941> (2022).
22. Kippenberger, S., Loitsch, S., Solano, F., Bernd, A. & Kaufmann, R. Quantification of Tyrosinase, TRP-1, and TRP-2 transcripts in human melanocytes by reverse Transcriptase-Competitive multiplex PCR – Regulation by steroid hormones. *J. Investig Dermatol.* **110**, 364–367. <https://doi.org/10.1038/jid.1998.1> (1998).
23. Kobayashi, T. et al. Tyrosinase related protein 1 (TRP1) functions as a DHICA oxidase in melanin biosynthesis. *Embo J.* **13**, 4261–4268. <https://doi.org/10.1002/j.1460-2075.1994.tb06925.x> (1994).
24. Watabe, H. et al. Regulation of tyrosinase processing and trafficking by organellar pH and by proteasome activity. *J. Biol. Chem.* **279**, 7971–7981. <https://doi.org/10.1074/jbc.M309714200> (2004).
25. Kobayashi, T. & Hearing, V. J. Direct interaction of tyrosinase with Tyrp1 to form heterodimeric complexes in vivo. *J. Cell. Sci.* **120**, 4261–4268. <https://doi.org/10.1242/jcs.017913> (2007).
26. Snyman, M., Walsdorf, R. E., Wix, Sophia, N. & Gill, J. G. The metabolism of melanin synthesis—From melanocytes to melanoma. *Pigment Cell. Melanoma Res.* **37**, 438–452. <https://doi.org/10.1111/pcmr.13165> (2024).
27. Eccles, M. R. et al. MITF and PAX3 play distinct roles in melanoma cell Migration; outline of a genetic switch theory involving MITF and PAX3 in proliferative and invasive phenotypes of melanoma. *Front. Oncol.* **3**, 229. <https://doi.org/10.3389/fonc.2013.00229> (2013).
28. Hartman, M. L. & Czyz, M. MITF in melanoma: mechanisms behind its expression and activity. *Cell. Mol. Life Sci.* **72**, 1249–1260. <https://doi.org/10.1007/s00018-014-1791-0> (2015).
29. Mo, X., Kazmi, H. R., Preston-Alp, S., Zhou, B. & Zaidi, M. R. Interferon-gamma induces melanogenesis via post-translational regulation of tyrosinase. *Pigment Cell. Melanoma Res.* **35**, 342–355. <https://doi.org/10.1111/pcmr.13036> (2022).
30. Newton, R. A., Cook, A. L., Roberts, D. W., Leonard, J. H. & Sturm, R. A. Post-transcriptional regulation of melanin biosynthetic enzymes by cAMP and Resveratrol in human melanocytes. *J. Invest. Dermatol.* **127**, 2216–2227. <https://doi.org/10.1038/sj.jid.5700840> (2007).
31. Ploper, D. & De Robertis, E. M. The MITF family of transcription factors: role in endolysosomal biogenesis, Wnt signaling, and oncogenesis. *Pharmacol. Res.* **99**, 36–43. <https://doi.org/10.1016/j.phrs.2015.04.006> (2015).
32. Ploper, D. et al. MITF drives endolysosomal biogenesis and potentiates Wnt signaling in melanoma cells. *Proc. Natl. Acad. Sci. USA.* **112**, E420–429. <https://doi.org/10.1073/pnas.1424576112> (2015).
33. Ambrosio, A. L., Boyle, J. A., Aradi, A. E., Christian, K. A. & Di Pietro, S. M. TPC2 controls pigmentation by regulating melanosome pH and size. *Proc. Natl. Acad. Sci. USA.* **113**, 5622–5627. <https://doi.org/10.1073/pnas.1600108113> (2016).
34. Bellono, N. W., Escobar, I. E. & Oancea, E. A melanosomal two-pore sodium channel regulates pigmentation. *Sci. Rep.* **6**, 26570. <https://doi.org/10.1038/srep26570> (2016).
35. Sulem, P. et al. Two newly identified genetic determinants of pigmentation in Europeans. *Nat. Genet.* **40**, 835–837. <https://doi.org/10.1038/ng.160> (2008).
36. Zhou, D. et al. Two-pore channel 2 is required for soluble adenylyl cyclase-dependent regulation of melanosomal pH and melanin synthesis. *Pigment Cell. Melanoma Res.* **37**, 656–666. <https://doi.org/10.1111/pcmr.13177> (2024).
37. Muller, M. et al. Gene editing and synthetically accessible inhibitors reveal role for TPC2 in HCC cell proliferation and tumor growth. *Cell. Chem. Biol.* **28**, 1119–1131. <https://doi.org/10.1016/j.chembiol.2021.01.023> (2021). e1127.
38. Pafumi, I. et al. Naringenin impairs Two-Pore channel 2 activity and inhibits VEGF-Induced angiogenesis. *Sci. Rep.* **7**, 5121. <https://doi.org/10.1038/s41598-017-04974-1> (2017).
39. Rebello, C. J. et al. Safety and pharmacokinetics of naringenin: A randomized, controlled, single-ascending-dose clinical trial. *Diabetes Obes. Metab.* **22**, 91–98. <https://doi.org/10.1111/dom.13868> (2020).
40. Huang, Y. C., Yang, C. H. & Chiou, Y. L. Citrus Flavanone naringenin enhances melanogenesis through the activation of Wnt/beta-catenin signalling in mouse melanoma cells. *Phytomedicine* **18**, 1244–1249. <https://doi.org/10.1016/j.phymed.2011.06.028> (2011).

Acknowledgements

This research project is supported by the Second Century Fund (C2F) Chulalongkorn University and the 90th Anniversary of Chulalongkorn University Fund (Ratchadaphiseksomphot Endowment Fund) Batch #51 Round 1/2022 Academic Year 2022 (Grant no. GCUGR1125651018D).

Author contributions

Conceptualisation, C.G. and W.D-E.; Formal analysis, P. P., R.T., R.H., C.A., and P.N.; Funding acquisition, W.D-E.; Investigation, P.P., R.T., R.H., C.A., and P.N.; Methodology, C.A., P.N., W.C., C.C., and C.G.; Resources, W.C., C.G., and W.D-E.; Supervision, W.D-E. and C.G.; Validation, C.A., W.C., C.C., C.G., and W. D-E.; Visualisation, P.P., R.T., R.H., C.A., P.N., and C.C.; Writing—original draft, P.P., R.T. and R.H.; Writing—review and editing, P.N., C.C., W.C., and C.G. All authors have read and agreed to the published version of the manuscript.

Declarations

Competing interests

The authors declare no competing interests.

Additional information

Supplementary Information The online version contains supplementary material available at <https://doi.org/10.1038/s41598-025-27629-y>.

Correspondence and requests for materials should be addressed to C.G. or W.D.

Reprints and permissions information is available at www.nature.com/reprints.

Publisher's note Springer Nature remains neutral with regard to jurisdictional claims in published maps and institutional affiliations.

Open Access This article is licensed under a Creative Commons Attribution-NonCommercial-NoDerivatives 4.0 International License, which permits any non-commercial use, sharing, distribution and reproduction in any medium or format, as long as you give appropriate credit to the original author(s) and the source, provide a link to the Creative Commons licence, and indicate if you modified the licensed material. You do not have permission under this licence to share adapted material derived from this article or parts of it. The images or other third party material in this article are included in the article's Creative Commons licence, unless indicated otherwise in a credit line to the material. If material is not included in the article's Creative Commons licence and your intended use is not permitted by statutory regulation or exceeds the permitted use, you will need to obtain permission directly from the copyright holder. To view a copy of this licence, visit <http://creativecommons.org/licenses/by-nc-nd/4.0/>.

© The Author(s) 2025